



## Short communication

## Importance of open pore structures with mechanical integrity in designing the cathode electrode for lithium–sulfur batteries



C.-S. Kim <sup>a</sup>, A. Guerfi <sup>a</sup>, P. Hovington <sup>a</sup>, J. Trottier <sup>a</sup>, C. Gagnon <sup>a</sup>, F. Baray <sup>a</sup>, A. Vijh <sup>a</sup>, M. Armand <sup>b</sup>, K. Zaghib <sup>a,\*</sup>

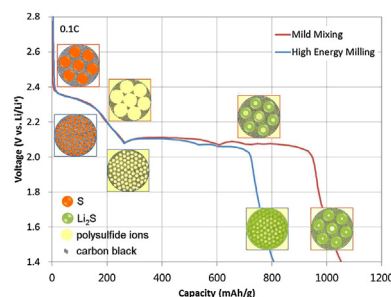
<sup>a</sup> Institut de Recherche d'Hydro-Québec (IREQ), 1800 Bd Lionel Boulet, Varennes, QC, Canada J3X 1S1

<sup>b</sup> CIC energiGUNE, Alava Technology Park, Albert Einstein, 4801510 MIÑANO Álava, Spain

## HIGHLIGHTS

- The Li/S cells can be improved by optimizing the electrode pore structure.
- The capacity of 1000 mAh g<sup>-1</sup> at 0.1 C was obtained.
- The stable capacity retention was of >700 mAh g<sup>-1</sup> after 200 cycles.
- At 0.5 C, it can be achieved with relatively high sulfur content of 68%.

## GRAPHICAL ABSTRACT



## ARTICLE INFO

## Article history:

Received 19 March 2013

Received in revised form

6 May 2013

Accepted 8 May 2013

Available online 16 May 2013

## Keywords:

Lithium/sulfur battery

Electrode process

Pore structure

Mechanical integrity

## ABSTRACT

The robustness of conductive networks and the accessibility of electrolyte into the network are important factors in designing the cathode electrode for lithium/sulfur (Li/S) batteries containing liquid electrolytes that involve liquid phase electrochemical reactions. We show that the performance of Li/S cells can be significantly improved by simply optimizing the electrode processing conditions to have open pore structures and mechanical integrity of the electrode architecture. It is demonstrated that the capacity of 1000 mAh g<sup>-1</sup> at 0.1 C and the stable capacity retention of >700 mAh g<sup>-1</sup> after 200 cycles at 0.5 C can be achieved with relatively high sulfur content of 68%. 417 Wh kg<sup>-1</sup> in specific energy and 623 Wh l<sup>-1</sup> in energy density are achievable with this new technology.

© 2013 Elsevier B.V. All rights reserved.

## 1. Introduction

With increasing demand for electric transportations that have competitive performance and affordable price, Li/S battery has attracted major attention as a battery system that can overcome the limitation of current lithium-ion technology [1,2]. The expectation

for Li/S battery is rationalized by the high theoretical capacity of sulfur (1672 mAh g<sup>-1</sup>), which outperforms any known solid cathode material, its natural abundance and environmental benefit [3].

Despite these attractive aspects, there are a number of technical challenges that have been hindering the commercialization of Li/S batteries for decades [4–6]. Firstly, sulfur and its insoluble reaction products (Li<sub>2</sub>S<sub>2</sub>/Li<sub>2</sub>S) are highly resistive in both electron and ion conduction, which limits the reversibility of the sulfur reaction (poor cycle life) and reduces the benefit of energy density because of the need for excessive amount of conductive additives (usually

\* Corresponding author.

E-mail address: [zaghib.karim@ireq.ca](mailto:zaghib.karim@ireq.ca) (K. Zaghib).

carbon). Secondly, the reaction intermediate, polysulfide ions ( $S_x^{2-}$ ,  $8 \leq x \leq 3$ ) are highly soluble in the liquid electrolytes causing a series of technical issues like low round-trip efficiency, severe self-discharge and parasitic reactions on lithium metal [7].

On the other hand, the high solubility of polysulfide plays a positive role as it allows better utilization of the highly insulating active material by greatly facilitating the contact between the active material and conductive matrix [4]. Without dissolution of polysulfide, only the portion of active material in intimate contact with carbon will be able to participate in the electrochemical reaction. In this regards, the solubility of polysulfide is an important requirement in the liquid electrolyte system [8,9].

Because the initial electrode morphology is not maintained when the soluble polysulfide ions are formed in the first discharge, the traditional approaches to make homogeneous electrode composition are not effective in manufacturing sulfur cathode electrodes. Even the stand-alone conductive carbon layers function effectively as cathode electrodes as long as they are used with the appropriate sulfur sources [10–13]. However, this approach does not address the challenge of lower volumetric energy density due to the presence of low density inactive layers in the cell. To take advantage of the high energy density of sulfur, improvements to Li/S batteries should consider the integrated design of electrodes. In this study, we show that the cell performance is strongly dependent on the electrode process conditions, and investigate the controlling factors influencing the correlation between performance and electrode structure.

## 2. Experimental

### 2.1. Powder treatment

Sulfur (Acros, >99%, refined), poly(ethylene oxide) (PEO, Polyscience, MW. 5,000,000) and poly(vinyl pyrrolidone) (PVP, DKS, MW.10,000) were dried under vacuum at 60 °C for 24 h before use. Ketjen Black (EC-600JD) was dried under vacuum at 120 °C for 24 h.

To make the sulfur–carbon composite, a dry mixture of sulfur and Ketjen Black (75:25 by weight) were placed in a stainless steel container filled with Ar gas and blended in a high energy mill (8000M Mixer/Mill, SPEX SamplePrep LLC) for 5–60 min. Stainless steel balls with 2 different diameters (2.5 mm + 4 mm by 1:1 ratio) were used to fill ~30% volume of the container. The operation was interrupted every 10 min to prevent overheating.

### 2.2. Electrode preparation and cell assembly

The binder solution of PEO (10 wt% in the mixed solvent of acetonitrile + toluene, 8:2 volume ratio) and PVP (10 wt% in absolute ethanol) was added to the as-prepared sulfur–carbon mixture with a ratio of 68:23:8:1 (sulfur:carbon black:PEO:PVP) after drying. Additional solvent (acetonitrile + toluene, 8:2 volume ratio) was added to the slurry to reach a viscosity of ~10,000 cP. Two different mixing conditions were employed to prepare the slurry. For mild mixing, a planetary centrifugal mixer (Thinky Mixer ARE-250) was used for 20 min. For aggressive mixing, a high energy mill (8000M Mixer/Mill, SPEX SamplePrep LLC) was used for 20 min. The slurry was coated on carbon-coated aluminum foil (15 µm) to a loading of 1–2 mg cm<sup>-2</sup> and carefully dried at 55 °C under mild vacuum.

CR2032 coin cells were assembled in a He-filled glove box using Celgard 3501 as separator and lithium foil (Hoshen, 200 µm) as anode. 0.12 ml of 1 M lithium bis(trifluoromethanesulfonyl)imide (LiTFSI) in a mixture of ethylene glycol–dimethyl ether (DME) and 1,3-dioxolane (DOX) (1:1 by volume ratio) was injected into the cell. No electrolyte additive was used.

### 2.3. Electrochemical test and characterization

Electrochemical tests were performed using a VMP cycler (Bio-Logic SAS) at 25 °C. To test the C-rate performance, constant current of 0.1–5 C (1 C = 1672 mA g<sup>-1</sup>) was applied for both charge and discharge in the voltage range between 1.4 V and 2.8 V vs. Li/Li<sup>+</sup>. Electrochemical impedance spectra were monitored in the frequency range from 200 kHz to 50 mHz with amplitude of 5 mV. Cycle life was tested at 0.5 C constant current in the voltage range between 1.4 V and 2.8 V vs. Li/Li<sup>+</sup>. Before the electrochemical tests, the cells were held at open circuit voltage for 12 h. Scanning electron microscopy (SEM) images were obtained using a field emission scanning electron microscope (Hitachi model S-4700).

## 3. Results and discussion

As the sulfur particles are easily deformed by both stress and heat, the original morphology of sulfur continuously changes during the electrode preparation process that includes mixing, coating, calendering and drying. In this study, two different mixing methods were employed to compare the change of morphology and its effects on the electrochemical performance. The first mixing method was done under the relatively mild condition using a planetary centrifugal mixer to preserve the original morphology of pristine materials. In this method, only wet mixing was performed for 20 min without additional treatment of powder. The second mixing method was carried out under more aggressive conditions using a high energy ball mill both in dry power and wet slurry to break down the agglomerates and enhance the sulfur-to-carbon contact. The dry milling was done for 5–60 min followed by wet milling for 20 min.

Fig. 1 shows the morphology of pristine sulfur, which is composed of loose agglomerates of 5–20 micron primary particles, and the sulfur–carbon composite made by dry ball-milling for 30 min. It appears that the sulfur particles are broken and partially melt during the milling process to form the sulfur–carbon composite where the contact area between carbon and sulfur is greatly enhanced. The red arrows in Fig. 1(d) indicate the domain of sulfur spread on the surface of sulfur–carbon composite.

The pores in the carbon particles are partially covered by sulfur in the sulfur–carbon composites, which leads to lower surface area compared with that of the constituent pristine materials. This is reflected in the reduced amount of solvent that is required to make the slurry. The blue line in Fig. 2 shows the content of non-volatile components (sulfur, carbon, binder) in the slurry that is required to reach a viscosity of ~10,000 cP. It appears that the amount of solvent is gradually reduced with milling time and the non-volatile content increases from 14% to 20%. The red line in Fig. 2 shows that the electrodes obtained at longer milling time have a lower porosity. The porosity was calculated by the difference between the specific volume of the electrodes and the true volume of the individual components.

The initial discharge and charge profiles measured with different electrodes are illustrated in Fig. 3. The initial discharge capacity is about 1100 mAh g<sup>-1</sup> at 0.1 C, irrespective of the electrode preparation conditions. The typical 2-step voltage plateaus corresponding to reduction from solid sulfur ( $S_8$ ) to soluble polysulfide ( $Li_2S_x$ ,  $x = 8–3$ ) at the 2.3 V region and the following reduction to insoluble lithium sulfides ( $Li_2S_2$  or  $Li_2S$ ) at the 2.1 V region are clearly evident. During the rest period (12 h) before starting discharge, the open circuit voltages (2.8–3 V) decrease due to self-discharge from partial solubility of sulfur in the liquid electrolyte. The results in the figure show that self-discharge is accelerated with increasing milling time, probably due to the enhanced exposure of sulfur to the electrolyte when it is in dispersed domains.

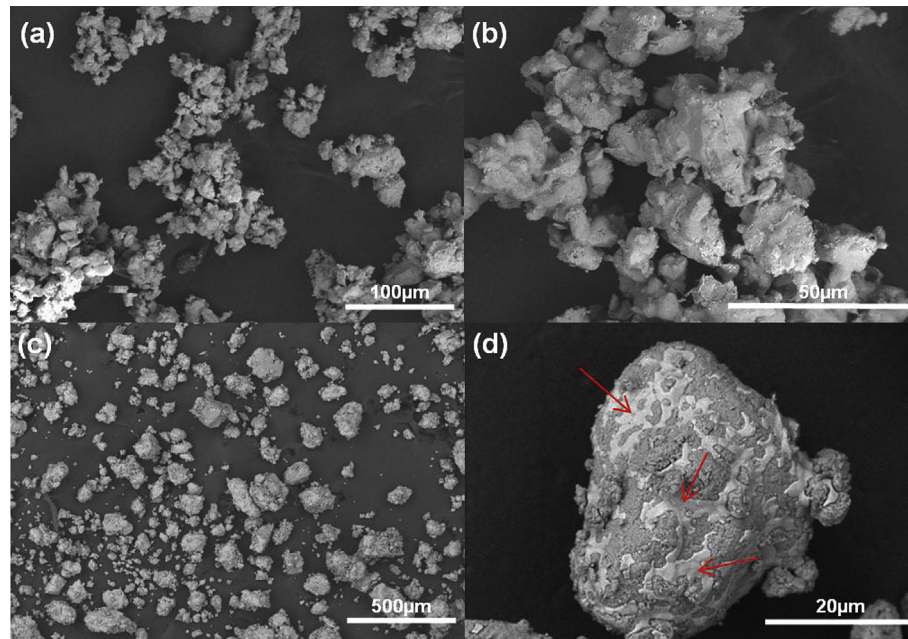


**Fig. 1.** SEM backscattered electrons images showing morphology change during the dry milling process. (a) and (b) Pristine sulfur particles. (c) and (d) Sulfur–carbon composites after dry ball-milling for 30 min. Red arrows indicate the domain of sulfur spread on the surface of sulfur–carbon composite. (For interpretation of the references to colour in this figure legend, the reader is referred to the web version of this article.)

Furthermore, the shuttle reactions at the 2.35 V region in the charging curves are more severe in electrodes obtained with longer milling time making the charging capacity much higher than those drained during the discharge step, which indicates that the dissolution of polysulfide ions and their reduction on lithium metal anode are facilitated in the sulfur–carbon composite. The magnified graph in the inset displays the trend of voltage peak at the beginning of charge. These voltage peaks are caused by polarization that is attributed to the accumulation of insoluble discharge products ( $\text{Li}_2\text{S}_2$ ,  $\text{Li}_2\text{S}$ ) during the later part of discharge in the 2.1 V region [4]. As the discharge products are highly insulating, the charge reaction of this material suffers from high polarization, but

once oxidation initiates, polarization instantly decreases by generation of soluble polysulfide ions. It appears in Fig. 3 that polarization by discharge product is more severe in electrodes obtained at longer milling time. The reduced porosity shown in Fig. 2, and the concentrated deposition on the electrode surface by accelerated polysulfide dissolution (as evidenced by lower coulombic efficiency in Fig. 3) could explain the higher passivation behavior of electrodes with longer milling time.

Fig. 4 shows the C-rate performance and cycle life of different electrodes. We tested 2–4 cells with the same electrode and the average values were displayed in the figure with error bars indicating standard deviations. All the cells in Fig. 4 exhibit fast capacity decay during the initial cycles, and the cells with electrodes

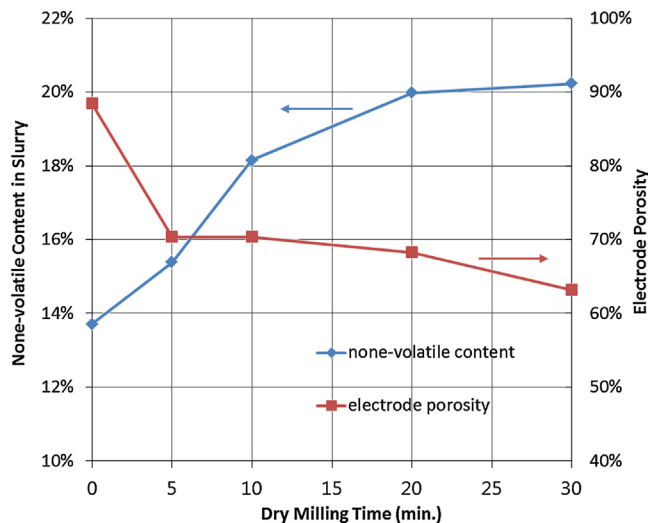


**Fig. 2.** Content of non-volatile components in the slurry and the electrode porosity, both as a function of the dry milling time. The slurry with longer milling time has lower solvent content, resulting in lower electrode porosity. (For interpretation of the references to colour in this figure legend, the reader is referred to the web version of this article.)

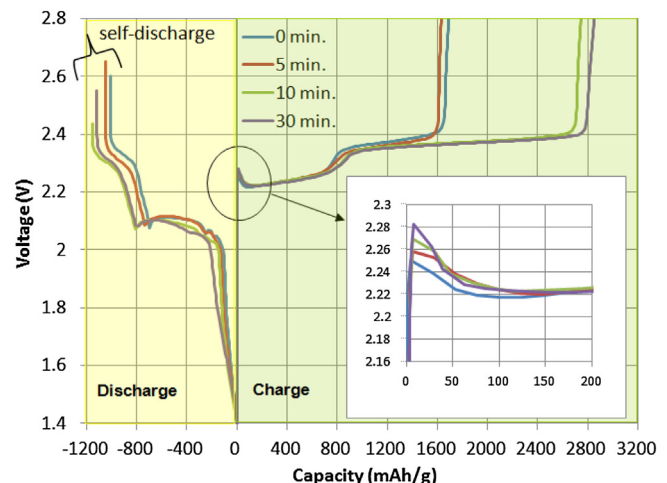


**Fig. 3.** Initial discharge and charge profiles for electrodes obtained with different mixing times. Sulfur–carbon composites show the accelerated self-discharge and severe shuttle behavior along with higher polarization at the beginning of the charge reaction.

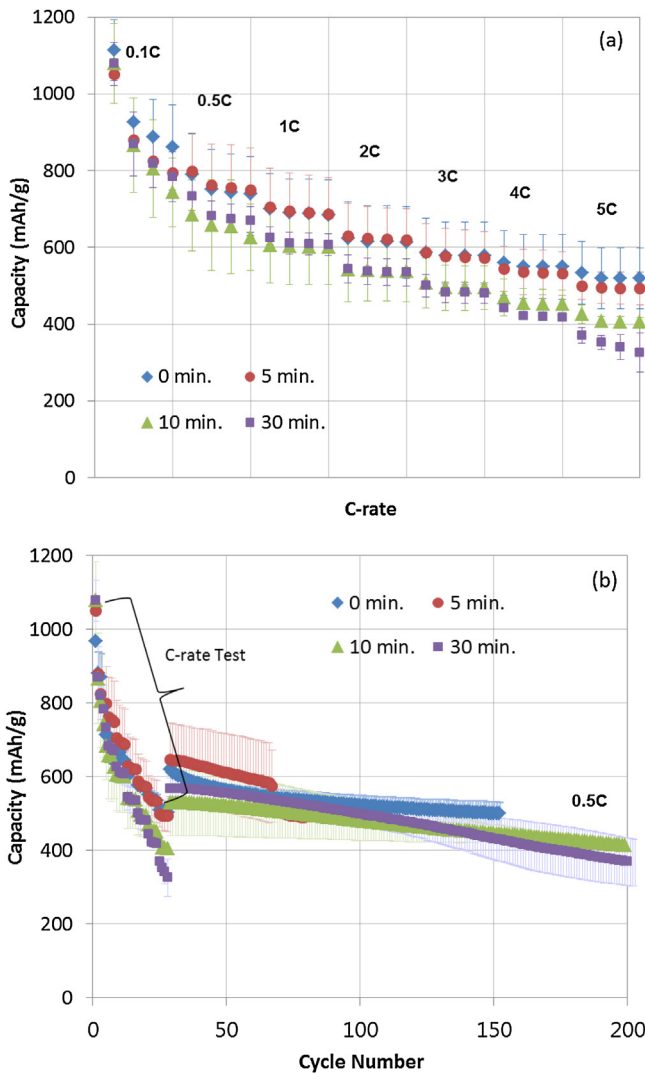


Fig. 4. (a) C-rate performance and (b) cycle life of electrodes obtained by dry milling for different times. The same charge and discharge current was used in the tests.

obtained from dry milling tend to have lower C-rate performance with steeper capacity decay. This result is well correlated with the higher polarization and lowered columbic efficiency shown in Fig. 3, which indicates that the enhanced contact between sulfur and carbon induced by high energy milling is not effective to improve the electrochemical performance in Li/S batteries. This is in agreement with the conclusion from literature reports that the initial morphology of sulfur does not make a difference once the active sulfur becomes soluble in the electrolyte [14].

In the sulfur cathode, the active sites are provided by the conductive carbons in direct contact with the electrolyte, and the electrode structural integrity is attributed to the mechanical strength of the carbon network. We expect that the pore structure derived by the packing arrangement of carbon particles is an important factor controlling the cell performance. The effect of porosity on performance was investigated by using electrodes that were calendered under different conditions. Fig. 5 shows the electrochemical performance of electrodes with different calendering conditions. Owing to the flexible nature of sulfur, the electrode density can be significantly increased to a value close to the true density ( $1.79 \text{ g cc}^{-1}$ ) of electrode. In the C-rate test, the electrodes with high density ( $1.7 \text{ g cc}^{-1}$ ) showed lower performance at high rate, while the electrodes with medium density ( $1-1.1 \text{ g cc}^{-1}$ )

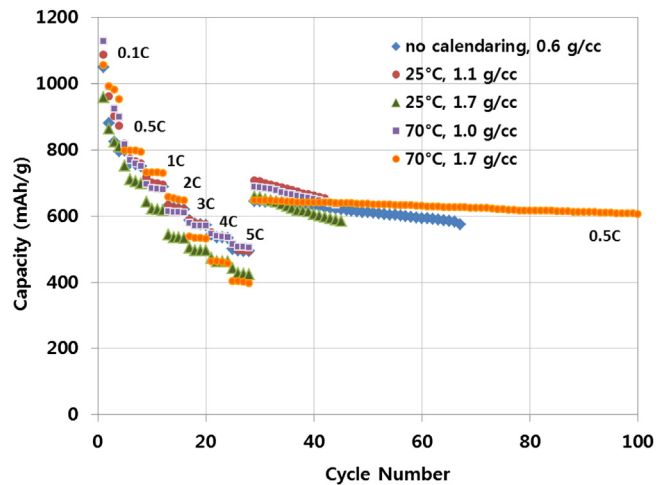


Fig. 5. C-rate performance and cycle life of electrodes obtained with different calendering conditions. The electrodes were prepared by dry milling for 5 min, followed by wet milling for 20 min. The calendering temperature and electrode density are listed in the figure.

showed little difference in performance. This implies that the electrode density can be enhanced without sacrificing power performance, as long as the pore structure allows easy access of active species in the conductive network. In the cycle life test, a remarkable improvement was observed with the high density electrode calendered at  $70^\circ\text{C}$  because the enhanced mechanical integrity of the electrode is able to accommodate the mechanical stress induced by the morphology change and severe volume expansion (78%) over the repeated cycles.

Electrodes prepared by different mixing conditions were calendered at  $70^\circ\text{C}$  to have the electrode density of  $1.7 \text{ g cc}^{-1}$  and their electrochemical performance was investigated. Fig. 6 shows that electrodes prepared by high energy milling exhibit negligible cycle life improvement by calendering. However, a significant improvement was found in the capacity retention of electrodes prepared in the mild mixing condition. To analyze the cause of this difference, the electrochemical impedance spectra were obtained at  $100 \text{ mAh g}^{-1}$  intervals during discharge, as indicated in Fig. 7(a). Fig. 7(b) and (c) shows the evolution of the impedance spectra

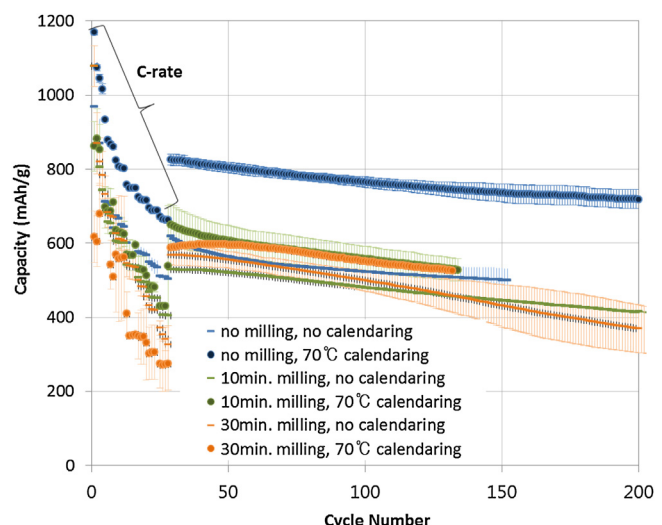
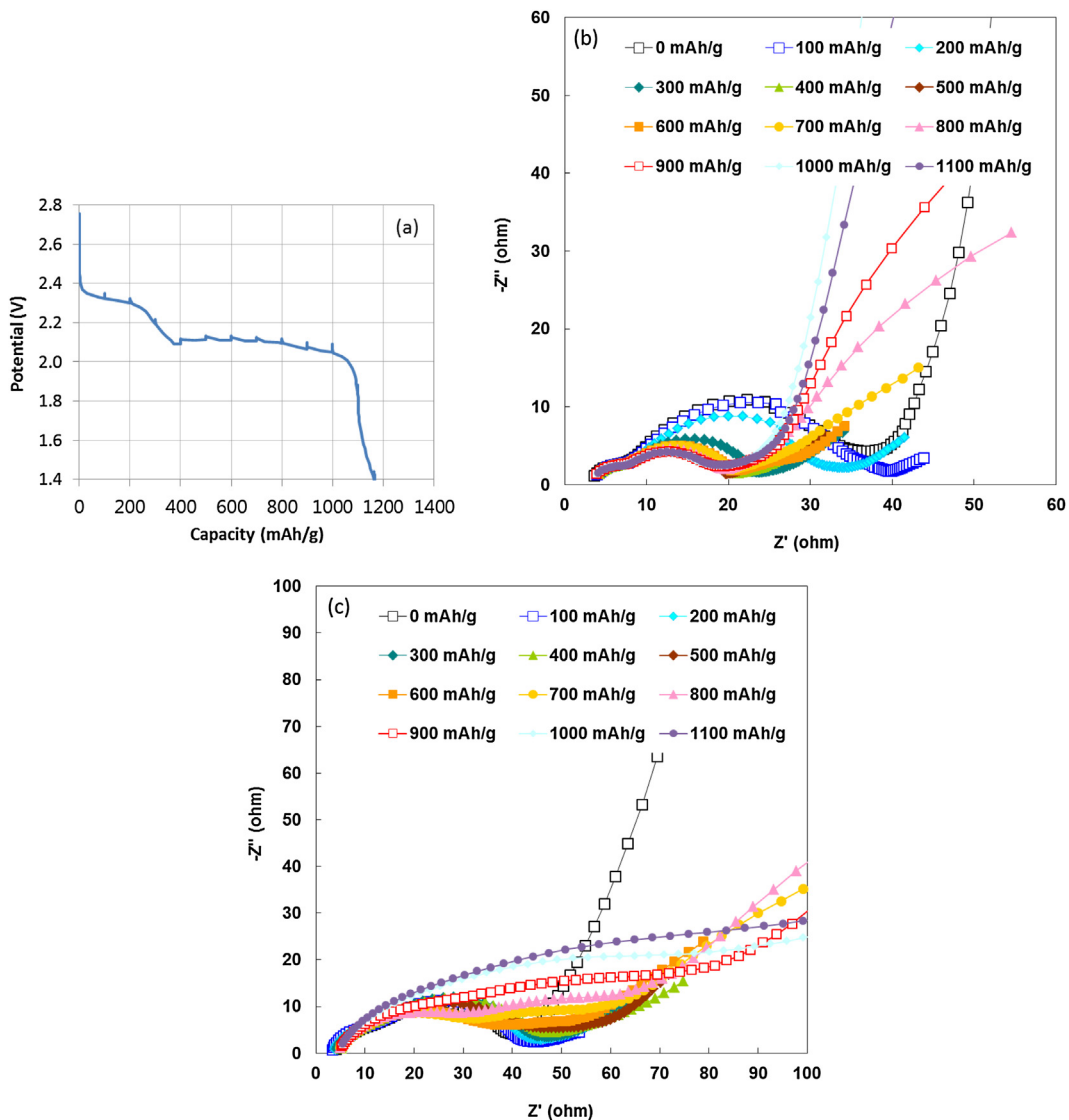


Fig. 6. The effect of high-temperature calendering ( $70^\circ\text{C}$ ) on the cycle life of electrodes prepared with different mixing conditions. The dry milling time and calendering condition are listed in the figure.

taken during the 2nd discharge at 0.1 C using electrodes obtained from different mixing conditions. Fig. 7(b) shows the typical Nyquist plot of a sulfur cathode that is composed of two depressed semi-circles and one straight or curved line [14–16]. The smaller semi-circle in the high frequency region is almost constant over the whole discharge reaction, while the larger semi-circle in the medium frequency range is affected by the depth of discharge. Although the assignment of the details in the Nyquist plot is still controversial, it is generally interpreted that the semi-circle in the medium frequency range corresponds to the charge transfer resistance and its relevant capacitance. It can be seen that the medium frequency semi-circle is significantly reduced in the early part of discharge in the 2.3 V region, and stabilized during the lower voltage plateau region at 2.1 V. This response indicates that the charge transfer resistance is greatly reduced by the transformation of solid sulfur to soluble polysulfides, owing to the enhanced active sites and facile accessibility of active species from the electrolyte. With the accumulation of insoluble discharge products ( $\text{Li}_2\text{S}_2/\text{Li}_2\text{S}$ ), the low frequency region shows serious Warburg impedance and a blocking behavior at the completion of discharge. Contrary to the

results in Fig. 7(b), the charge transfer resistance in Fig. 7(c) is not reduced noticeably in the 2.3 V discharge region, which indicates that the dissolution of solid sulfur does not lead to enhanced electrochemical reactions. Furthermore, as the reaction approaches the end of discharge, the charge transfer resistance significantly increases, forming the extended arc in the low frequency range. This demonstrate that the active sites in the ball-milled electrode are not easily accessible to electrolytes and seriously passivated by the formation of  $\text{Li}_2\text{S}_2/\text{Li}_2\text{S}$ , which is caused by the difference in the pore structure. The electrode prepared by mild mixing condition contains larger sulfur domains (bright region in Fig. 8(a) and (b)) that are transformed to open pores in the cell, allowing facile access of the electrolyte. On the other hand, the electrode made by aggressive mixing conditions is composed of more uniformly dispersed sulfur–carbon composite (as shown in Figs. 1(d) and 8(c) and (d)) so the pore size is smaller with higher tortuosity, inhibiting electrolyte penetration into the electrode structure. This confirms the premise that the accessibility of active species through the well-developed open pore structure is conductive to achieving high capacity and stable cycle life of sulfur cathode electrode.



**Fig. 7.** (a) Discharge profile showing the impedance measurement points. Evolution of the impedance spectra for (b) the electrode prepared by mild mixing (planetary centrifugal mixing for 20 min without ball-milling); and (c) the electrode obtained by aggressive mixing (dry ball-milling for 30 min, followed by wet ball-milling for 20 min). Both electrodes were calendered at 70 °C.

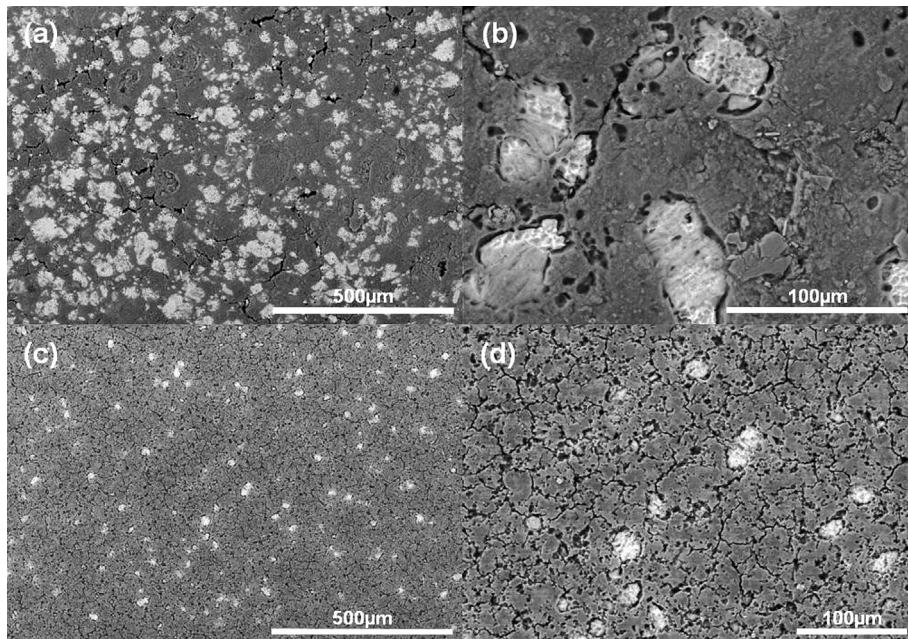


**Fig. 8.** SEM backscattered electrons images of the electrodes prepared by different mixing process. (a) and (b) are from mild mixing; and (c) and (d) are from aggressive mixing.

#### 4. Conclusions

In this study, we achieved improved cell performance by optimizing the electrode preparation process using high surface carbon black. The results showed that the mild mixing conditions are beneficial for producing favorable pore structures, and high-temperature calendering is effective in enhancing the electrode integrity, as long as the open pore structure is maintained. The initial capacity  $>1000 \text{ mAh g}^{-1}$  at 0.1 C condition and the stable capacity retention  $>80\%$  after 200 cycles were obtained using commercial sulfur material without any electrolyte additive. 417 Wh kg $^{-1}$  in specific energy and 623 Wh l $^{-1}$  in energy density are achievable with this new technology.

#### References

- [1] X. Ji, L.F. Nazar, *J. Mater. Chem.* 20 (2010) 9821–9826.
- [2] A. Manthiram, Y. Fu, Y.-S. Su, *Acc. Chem. Res.* (2012), <http://dx.doi.org/10.1021/ar300179v>.
- [3] R.D. Rauh, K.M. Abraham, G.F. Pearson, J.K. Surprenant, S.B. Brummer, *J. Electrochem. Soc.* 126 (1979) 523–527.
- [4] S.S. Zhang, *J. Power Sources* 231 (2013) 153–162.
- [5] V.S. Kolosnitsyn, E.V. Karaseva, *Russ. J. Electrochem.* 44 (2006) 548–552.
- [6] M.-K. Song, E.J. Cairns, Y. Zhang, *Nanoscale* (2013), <http://dx.doi.org/10.1039/C2NR33044J>.
- [7] Y.V. Mikhaylik, J.R. Akridge, *J. Electrochem. Soc.* 151 (2004) A1969–A1976.
- [8] S.-E. Cheon, K.-S. Ko, J.-H. Cho, S.-W. Kim, E.-Y. Chin, H.-T. Kim, *J. Electrochem. Soc.* 150 (2003) A800–A805.
- [9] Z. Lin, Z. Liu, W. Fu, N.J. Dudney, C. Liang, *Adv. Funct. Mater.* (2012) 1–6.
- [10] E. Peled, A. Gorenstein, M. Segal, Y. Sternberg, *J. Power Sources* 26 (1989) 269–271.
- [11] Y.-S. Su, A. Manthiram, *Chem. Commun.* 48 (2012) 8817–8819.
- [12] S.S. Zhang, D.T. Tran, *J. Power Sources* 211 (2012) 169–172.
- [13] C. Barchasz, F. Mesquich, J. Dijon, J.-C. Leprière, S. Patoux, F. Alloin, *J. Power Sources* 211 (2012) 19–26.
- [14] C. Barchasz, J.-C. Leprière, F. Alloin, S. Patoux, *J. Power Sources* 199 (2012) 322–330.
- [15] L. Yuan, X. Qui, L. Chen, W. Zhu, *J. Power Sources* 189 (2009) 127–132.
- [16] Z. Deng, Z. Zhang, Y. Lai, J. Liu, J. Li, Y. Liu, *J. Electrochem. Soc.* 160 (2013) A553–558.